

# The Use of Fluoroproline in MUC1 Antigen Enables Efficient Detection of Antibodies in Patients with Prostate Cancer

Víctor J. Somovilla,<sup>†,‡,□</sup> Iris A. Bermejo,<sup>†,□</sup> Inês S. Albuquerque,<sup>§,□</sup> Nuria Martínez-Sáez,<sup>†,‡</sup> Jorge Castro-López,<sup>||</sup> Fayna García-Martín,<sup>⊥</sup> Ismael Compañón,<sup>†</sup> Hiroshi Hinou,<sup>⊥</sup> Shin-Ichiro Nishimura,<sup>⊥</sup> Jesús Jiménez-Barbero,<sup>#</sup> Juan L. Asensio,<sup>¶</sup> Alberto Avenoza,<sup>†</sup> Jesús H. Busto,<sup>†</sup> Ramón Hurtado-Guerrero,<sup>||,△</sup> Jesús M. Peregrina,<sup>†</sup> Gonçalo J. L. Bernardes,<sup>\*,§,▽</sup> and Francisco Corzana<sup>\*,†</sup>

<sup>†</sup>Departamento de Química, Universidad de La Rioja, Centro de Investigación en Síntesis Química, 26006 Logroño, Spain

<sup>‡</sup>Department of Chemical Biology and Drug Discovery, Utrecht Institute for Pharmaceutical Sciences, Bijvoet Center for Biomolecular Research, Utrecht University, Universiteitsweg 99, Utrecht, The Netherlands

<sup>§</sup>Instituto de Medicina Molecular, Faculdade de Medicina da Universidade de Lisboa, Avenida Professor Egas Moniz, 1649-028, Lisboa, Portugal

<sup>||</sup>Institute of Biocomputation and Physics of Complex Systems (BIFI), University of Zaragoza, BIFI-IQFR (CSIC), Zaragoza, Spain

<sup>⊥</sup>Graduate School and Faculty of Advanced Life Science, Field of Drug Discovery Research, Hokkaido University, N21 W11, Sapporo 001-0021, Japan

<sup>#</sup>(i) CIC bioGUNE, Bizkaia Technology Park, Building 801A, 48170 Derio, Spain; (ii) Ikerbasque, Basque Foundation for Science, Maria Diaz de Haro 13, 48009 Bilbao, Spain; (iii) Department of Organic Chemistry II, Faculty of Science & Technology, University of the Basque Country, 48940 Leioa, Spain

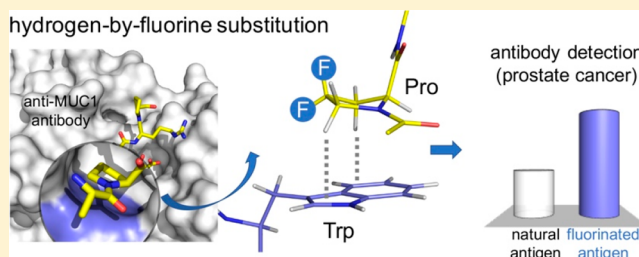
<sup>¶</sup>Instituto de Química Orgánica General, IQOG-CSIC, 28006 Madrid, Spain

<sup>△</sup>Fundación ARAID, 50018 Zaragoza, Spain

<sup>▽</sup>Department of Chemistry, University of Cambridge, Lensfield Road, CB2 1EW Cambridge, U.K.

## Supporting Information

**ABSTRACT:** A structure-based design of a new generation of tumor-associated glycopeptides with improved affinity against two anti-MUC1 antibodies is described. These unique antigens feature a fluorinated proline residue, such as a (4*S*)-4-fluoro-*L*-proline or 4,4-difluoro-*L*-proline, at the most immunogenic domain. Binding assays using biolayer interferometry reveal 3-fold to 10-fold affinity improvement with respect to the natural (glyco)peptides. According to X-ray crystallography and MD simulations, the fluorinated residues stabilize the antigen–antibody complex by enhancing key CH/ $\pi$  interactions. Interestingly, a notable improvement in detection of cancer-associated anti-MUC1 antibodies from serum of patients with prostate cancer is achieved with the non-natural antigens, which proves that these derivatives can be considered better diagnostic tools than the natural antigen for prostate cancer.



## INTRODUCTION

MUC1 is a glycoprotein overexpressed in around 80% of human cancers.<sup>1–3</sup> It consists of an extracellular domain that comprises a variable number (20 to 125) of tandem repeat regions formed by 20 amino acids (His-Gly-Val-Thr-Ser-Ala-Pro-Asp-Thr-Arg-Pro-Ala-Pro-Gly-Ser-Thr-Ala-Pro-Ala). This domain includes five potential *O*-glycosylation sites, with three threonine (Thr) and two serine (Ser) residues. While in healthy cells, the MUC1 backbone displays complex oligosaccharides, in tumors it is decorated with basic, truncated carbohydrates. Consequently, different tumor-associated carbohydrate antigens (TACAs), such as the Tn determinant ( $\alpha$ -*O*-GalNAc-Ser/Thr),

become exposed and are involved in triggering immune responses.<sup>4–7</sup> Because of this unique feature, extensive efforts have been made toward the development of cancer vaccines based on MUC1 fragments.<sup>8–12</sup>

In addition, over the years, several studies have demonstrated that circulating anti-MUC1 antibodies in serum may be used as a favorable prognosis for patients with early breast and pancreatic cancer because these antibodies can limit tumor outgrowth and dissemination.<sup>13–18</sup> Consequently, efforts have

Received: September 4, 2017

Published: November 22, 2017

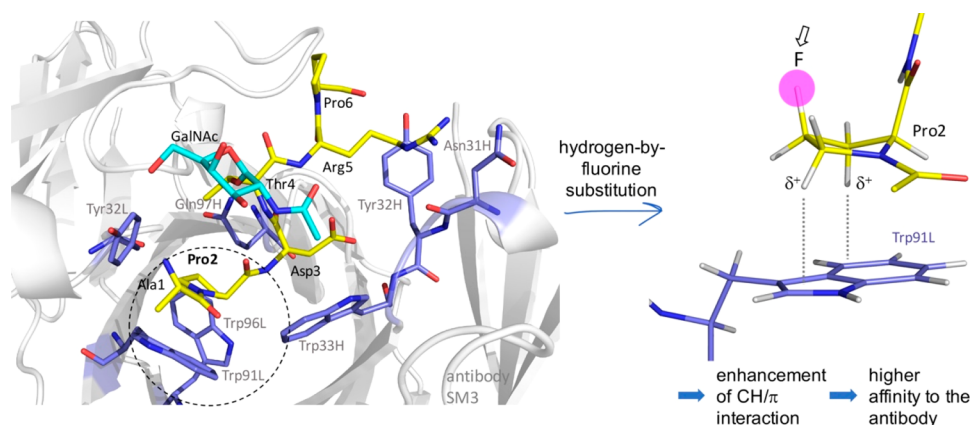


**Figure 1.** Hydrogen-by-fluorine Pro replacement strategy to improve antibody–antigen affinity. Crystal structure of glycopeptide APDT( $\alpha$ -O-GalNAc)RP in complex with antibody SM3 (pdb ID: 5a2k) together with the strategy proposed in this work to design effective antigens based on MUC1.

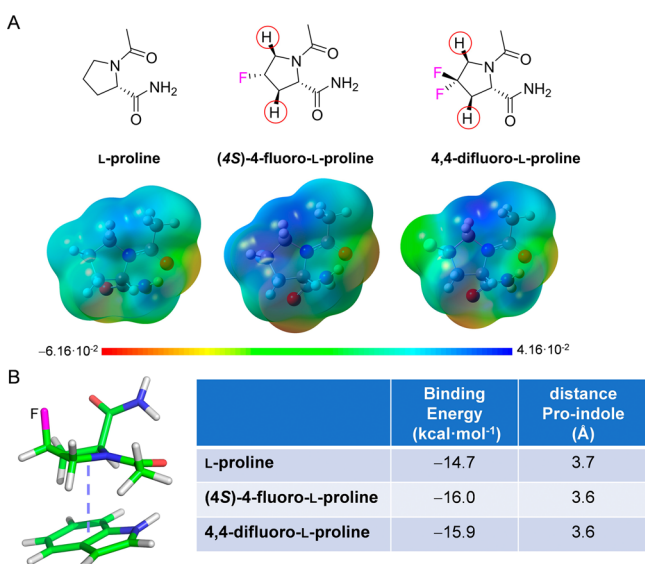


**Figure 2.** Effect of fluorine atoms on the electrostatic potential and on CH/ $\pi$  stability. (A) Electrostatic potential surfaces (in au) calculated at the M06-2X/6-31+G(d,p) level in a vacuum, showing the *re* faces of the Pro derivatives. Blue/red indicates positive/negative potentials. (B) Binding energy calculated at the M06-2X/6-31+G(d,p) level in a vacuum for the three Pro derivatives with an indole residue, together with the optimized distance Pro–indole for the complexes.

been devoted toward the rational design of MUC1-based antigens to be used as diagnostic tools for detection of anti-MUC1 antibodies in human serum. Unfortunately, so far, a commercial assay for early cancer diagnosis based on the detection of anti-MUC1 antibodies in human serum remains unavailable. However, significant advances toward this aim were reported by Wang and co-workers,<sup>19</sup> where they described an assay based on a recombinant MUC1 protein that contained six MUC1 tandem repeats and was effective in detecting anti-MUC1 antibodies in serum from patients. More recently, a chimera containing both MUC1 and human epidermal growth factor receptor-2 (HER2), whose overexpression is associated with malignancy in breast cancer, has been developed for detection of antibodies against MUC1 or HER2 in human serum.<sup>20</sup> It should be noted that, in these examples, antibody detection relies on unmodified naturally occurring antigens.

Alternatively, fine-tuning of antibody/antigen interactions by exploiting non-natural, synthetically designed antigen modifications

holds great potential in the development of diagnostic detection systems with improved selectivity and sensitivity. This strategy demands a precise understanding of the molecular basis of the antigen–antibody recognition process. In this regard, recent progress unveiled subtle molecular details of the antibody/antigen interaction,<sup>21,22</sup> paving the way to the structure-based design of synthetic antigens with improved potential value in diagnosis and detection. In this context, it has been shown that most anti-MUC1 antibodies display a significant affinity to peptide fragments containing the APDTRP sequence,<sup>23</sup> which consequently represents an attractive target for lead optimization.

Our group has recently described the X-ray structure of a short peptide bearing the sequence APDT( $\alpha$ -O-GalNAc)RP in complex with the SM3,<sup>22</sup> which is a therapeutic antibody used in the treatment of cancer.<sup>21</sup> According to these data, the nonterminal Pro residue plays a central role in the stabilization of the antibody/antigen complex, stacking against aromatic units of Trp91L, Trp96L, and Tyr32L (Figure 1). This observation explains why a proline residue at this position of the antigen is indeed essential for the binding of various anti-MUC1 antibodies.<sup>24</sup> Interestingly, recent studies have shown that CH/ $\pi$  bonds can be significantly enhanced by simply increasing the polarization of the interacting CH moieties.<sup>25–28</sup> In the present work, this effect could be achieved by attaching highly electronegative fluorine atoms to specific positions of the proline scaffold. Therefore, we hypothesized that the replacement of the nonterminal proline residue of the antigen by a non-natural proline derivative, such as (4S)-4-fluoro-L-proline or 4,4-difluoro-L-proline, should enhance antigen–antibody affinity (Figure 1).

Here, we designed and synthesized various MUC1 antigens that featured a hydrogen-by-fluorine substitution at that proline residue that displayed enhanced affinity to two anti-MUC1 antibodies. By combining molecular dynamic (MD) simulations and X-ray crystallography, we provide an explanation of the superior affinity of our derivatives toward two antibodies, which relies on stronger CH/ $\pi$  interactions. Finally, we demonstrate that these novel derivatives are more efficient than natural antigens in detecting low concentrations of circulating anti-MUC1 antibodies in human serum of patients with prostate cancer (adenocarcinoma and benign prostatic hyperplasia).

## RESULTS AND DISCUSSION

To provide theoretical support for the hypothesis depicted in Figure 1, we calculated the electrostatic potential surface of the

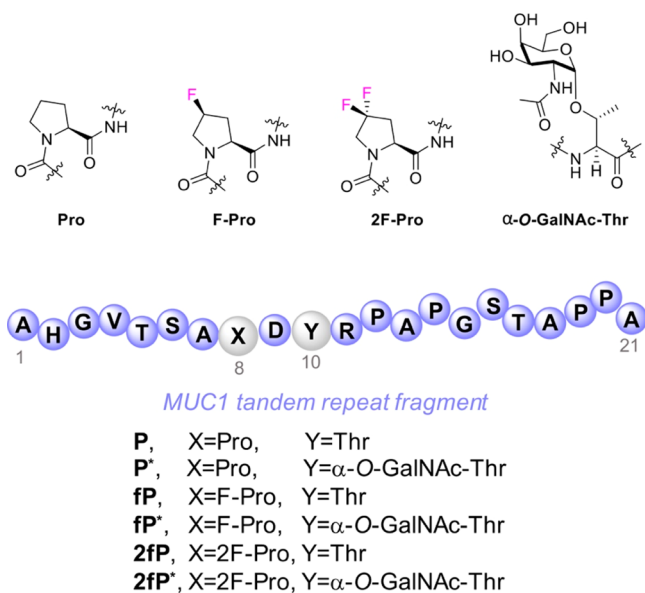


**Figure 3.** MUC1-like peptides and glycopeptides synthesized and studied in this work.

proline and its mono- and difluorinated derivatives shown in Figure 2A. In a second step, their interaction energies with an indole ring were evaluated at the M06-2X/6-31+G(d,p) level of theory.<sup>29</sup> The obtained relative energies were in agreement with our rational design and showed that the fluorinated residues displayed an enhanced positive partial charge on the CH/ $\pi$  donor methylene fragments (highlighted with a red circle in Figure 2A). As a result, the interacting proline face displays a

significantly larger electrostatic potential even for the mono-substituted derivative (4S)-4-fluoro-L-proline. This polarization effect is reflected in the theoretical interaction energies, with complex stabilizations larger than 1 kcal/mol (Figure 2B).

With these data in hand, we decided to synthesize a series of peptides and glycopeptides comprising the tandem repeat sequence of MUC1 (Figure 3) both fluorinated and nonfluorinated at position 8. The synthesis of all these derivatives was conducted using microwave-assisted solid phase peptide synthesis (MW-SPPS), employing a Rink amide MBHA resin and Fmoc-protected amino acids and using our reported protocol<sup>30</sup> (Supporting Information).

We then evaluated the impact of the hydrogen-by-fluorine substitutions on the antigen association to antibody scFv-SM3<sup>22</sup> using biolayer interferometry (BLI). Although both natural peptide **P** and glycopeptide **P\*** act as antigens, it has been observed that the latter displays better affinity than the naked peptide (Figure 4A).<sup>22,23</sup> This trend is also noted for the non-natural derivatives. To our delight, surrogates **fP\*** and **2fP\***, which contain a (4S)-4-fluoro-L-proline or a 4,4-difluoro-L-proline at position 8, respectively, showed the best affinity, with ca. 3-fold enhancement with respect to the natural **P\*** and 1 order of magnitude regarding natural peptide **P**. In parallel, we performed microarray assays<sup>31,32</sup> to determine the affinity of these MUC1 variants with commercially available antibodies SM3 and VU-3C6<sup>23</sup> (Figure 4B). The results obtained from the microarray experiments were in line with the BLI data, showing a clear increase in binding affinity for the non-natural variants. This result may indicate that both SM3 and VU-3C6 antibodies recognize the antigen with an equivalent binding mode.

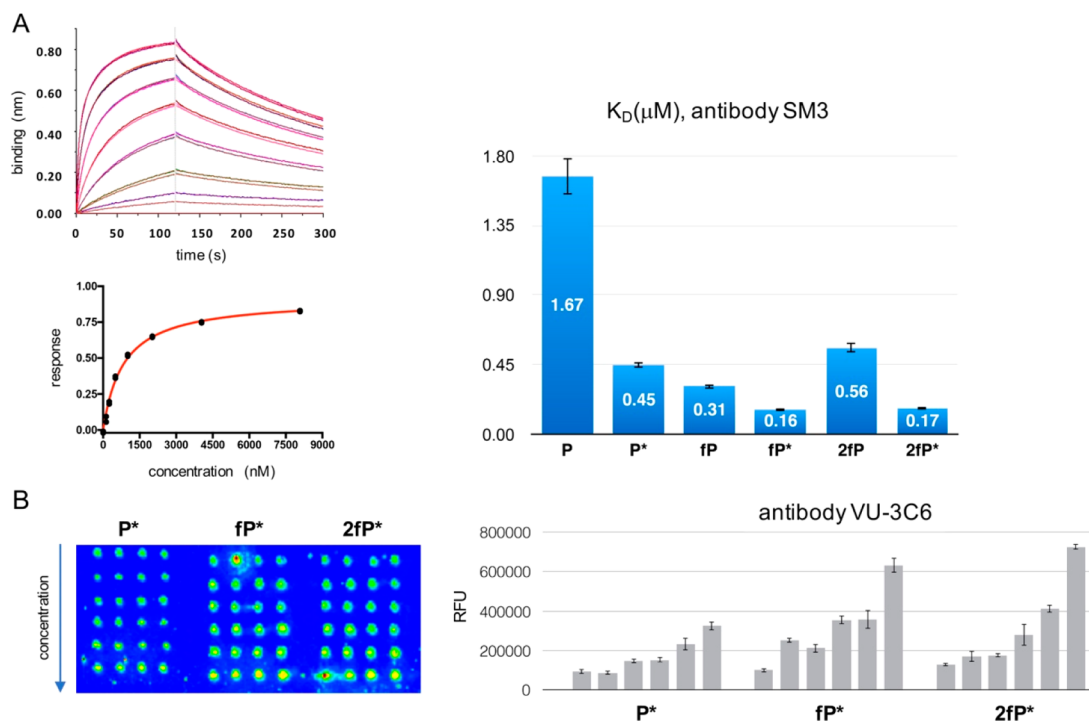


**Figure 4.** Binding of the glycopeptides to anti-MUC1 antibodies. (A) BLI curves and fit obtained for glycopeptide **fP\*** and antibody scFv-SM3, together with the  $K_D$  constants derived from BLI experiments for all studied MUC1-related compounds. (B) Interaction of the anti-MUC1 antibody VU-3C6 with the glycopeptides using a microarray platform. Compounds were printed onto an aminoxy-functionalized microarray in quadruplicate. Relative fluorescence units (RFU) due to the binding of the Cy3-labeled secondary antibody were measured and represented as mean values in a bar chart (see Supporting Information for experimental details).

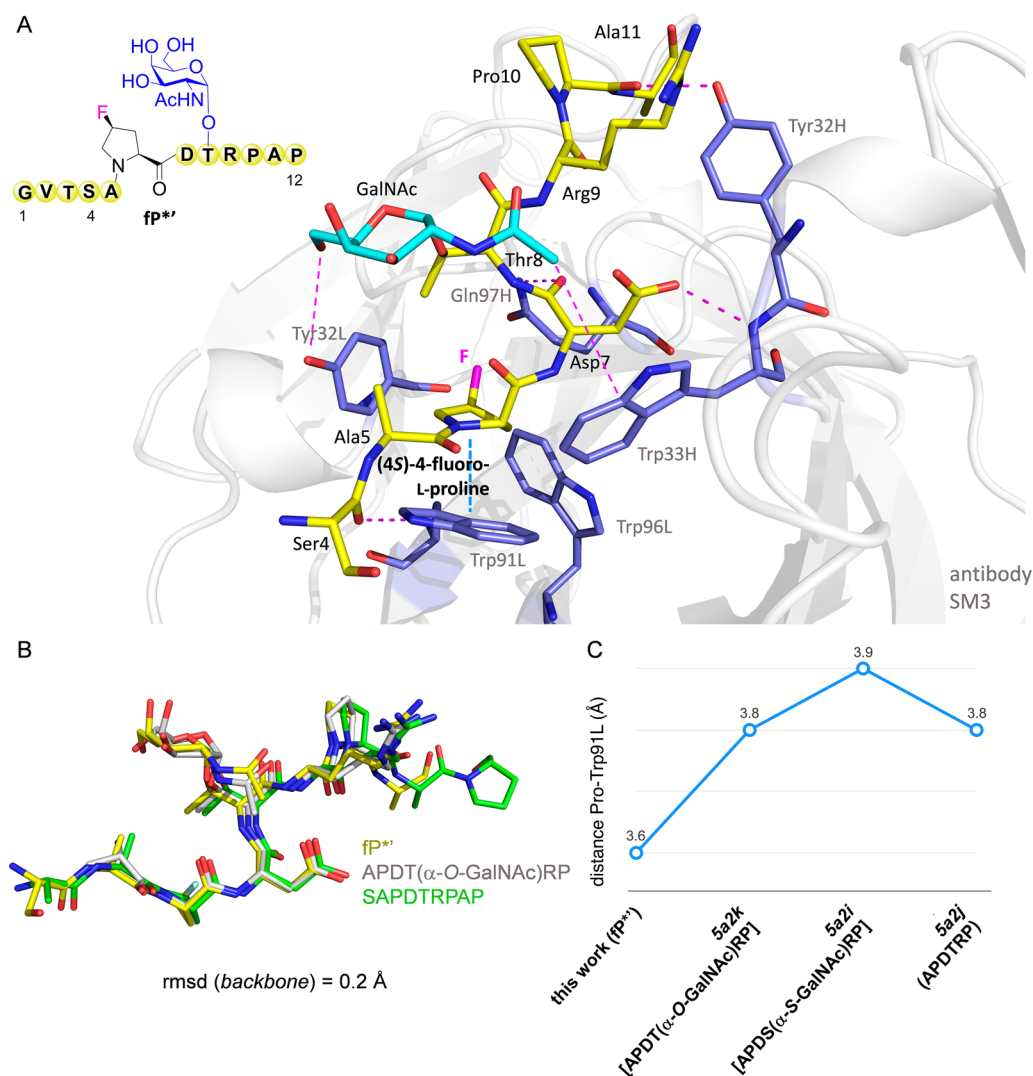


**Figure 5.** Crystal structure of  $fP^{**}$  bound to scFv-SM3. (A) Key binding interactions of glycopeptide  $fP^{**}$  with scFv-SM3 mAb, as observed in the X-ray crystal structure (pdb ID: 5OWP). Peptide backbone carbon atoms are shown in yellow. GalNAc carbon atoms are shown in cyan. Carbon atoms of key residues of SM3 are in slate. The antibody is shown as gray ribbons. Pink dashed lines indicate hydrogen bonds between peptide backbones and SM3 antibody. It is important to note that only residues SAPDTRP of the peptide could be resolved, presumably due to the higher flexibility of the rest of the amino acids. (B) Superposition of the peptide backbone of glycopeptides  $fP^{**}$  and APDT( $\alpha$ -O-GalNAc)RP, together with SAPDTRPAP peptide<sup>21</sup> in complex with SM3. The root-mean-square deviation (rmsd) of the backbone is shown. (C) Experimental distances Pro–Trp91L obtained from X-ray structures of various MUC1-like derivatives in complex with antibody SM3.

To fully validate our molecular design, we carried out detailed structural studies on our fluorinated antigens in complex with the antibody SM3. To this purpose, we synthesized a simplified variant of glycopeptide  $fP^{**}$ , comprising the sequences GVTSA $fP^{**}$ RPAP and denoted as  $fP^{**}$  throughout the Article. High-quality crystals of  $fP^{**}$  in complex with scFv-SM3 were obtained, which enabled the acquisition of a structure at high resolution ( $<2.0$  Å, Figure 5A and Supporting Information). Crystallographic analysis revealed that the conformation of the glycopeptide was almost identical to that found for peptide SAPDTRPAP and for glycopeptide APDT( $\alpha$ -O-GalNAc)RP in complex with the same antibody.<sup>21,22</sup> This outcome suggests that the incorporation of a fluorine atom at the proline residue does not significantly modify the structure of the peptide in the bound state (Figure 5B). Consequently, the antigen–antibody hydrogen-bonding network is identical to that found in the previously reported complexes.<sup>21,22</sup> The obtained results also indicate that GalNAc glycosylation does not have an influence

on the accommodation of the key proline residue (compare 5a2k and 5a2j in Figure 5C). In fact, the glycosidic linkage adopts the expected exoanomeric/syn conformation, with  $\phi$  and  $\psi$  values of  $\sim 68$  and  $91^\circ$ , respectively. This conformation is similar to that found for a Tn-glycopeptide in complex with SM3 (pdb ID: 5a2k)<sup>22</sup> and allows the formation of an intermolecular hydrogen bond between the hydroxymethyl group of GalNAc and the side chain of Tyr32L of the antibody. Moreover, the *N*-acetyl group of the sugar stacks with the aromatic ring of Trp33H, which provides the driving force for the observed selectivity of SM3 for GalNAc-containing antigens. Despite all these similarities, the obtained crystallographic coordinates revealed a subtle but crucial modification with previously reported structural data. Markedly, the observed distance between the center of the (4S)-4-fluoro-L-proline ring and Trp91L was significantly smaller than that observed for the Pro–Trp pairs in other complexes (Figure 5C). This result provides further support to our premise, strongly suggesting that

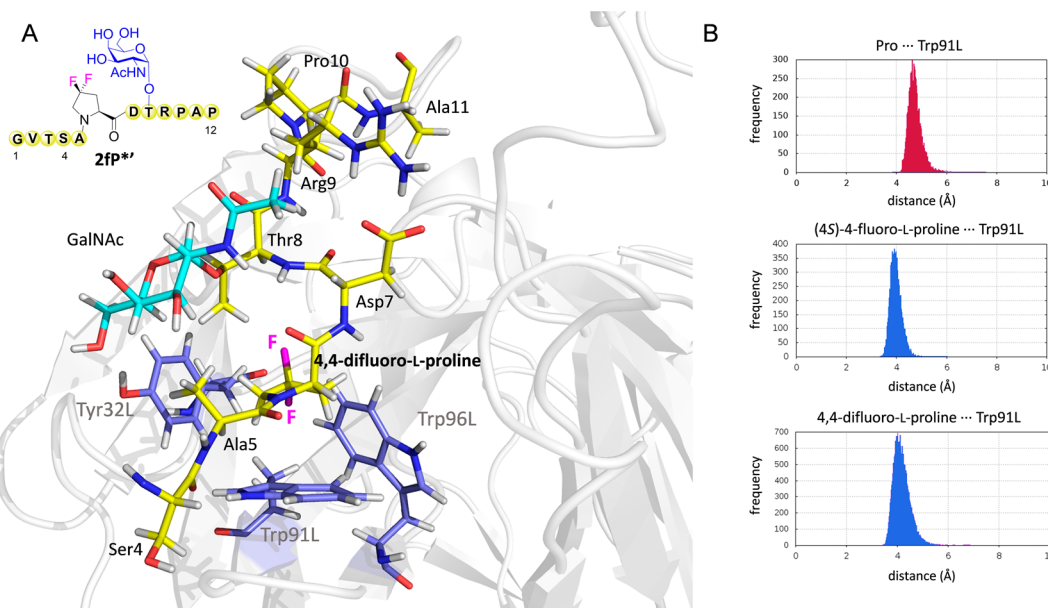


**Figure 6.** MD simulations of glycopeptide **2fP\*** in complex with scFv-SM3. (A) Representative frame of the 200 ns MD simulations performed on **2fP\*** in complex with antibody scFv-SM3. Only peptide fragment Ser4-Ala11 is shown for clarity. Peptide backbone carbon atoms are shown in yellow. GalNAc carbon atoms are shown in cyan. Carbon atoms of key residues of SM3 are in slate. The antibody is shown as gray ribbons. (B) Distance distribution of Pro–Trp91L obtained from 200 ns MD simulations for glycopeptides **P\*** (upper panel), **fP\*** (middle panel), and **2fP\*** (lower panel) bound to the antibody SM3.

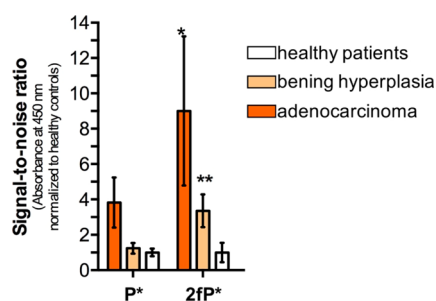


**Figure 7.** Detection of circulating anti-MUC1 antibodies in serum of patients presenting benign and malignant prostate cancer. Binding affinity of human circulating antibodies against MUC1 (**P\***) and synthetic variant **2fP\***, in the context of prostate adenocarcinoma and benign prostatic hyperplasia. Bars show average  $\pm$  standard error of the mean of absorbance values normalized to healthy controls. All groups were compared to **P\*** using Wilcoxon matched-pairs signed rank test; \* $p < 0.05$ ; \*\* $p < 0.02$  (see Supporting Information for details).

the improvement in the proline/tryptophan stacking accounts for the increased stability of the complexes formed by the non-natural fluorinated antigens.

The influence exerted by proline fluorination on the antigen/SM3 complexes was also analyzed by MD simulations. Thus, we collected 200 ns trajectories on **2fP\*** and **fP\*** bound to scFv-SM3 (Figure 6A). MD simulations on the reduced versions of natural glycopeptide (**P\***) complexed to the antibody were also conducted for comparative purposes. According to these theoretical data, the three complexes were stable through the simulations. Most importantly, a shorter distance between Pro and Trp91L was found for derivative **fP\*** (with a distance Pro–Trp91L =  $4.0 \pm 0.4$  Å), in agreement with the X-ray structure described in Figure 5, and for compound **2fP\*** (distance Pro–Trp91L =  $4.1 \pm 0.6$  Å). In contrast, the distance found for the natural glycopeptide **P\*** was  $4.7 \pm 0.4$  Å. In summary, both experimental and theoretical

data confirm the validity of our design and show that improving proline/tryptophan stacking-type interaction through simple hydrogen-by-fluorine substitutions represents a simple way to stabilize the antigen/antibody complex. These results hint that the tailored fluorinated MUC1 glycopeptides can be employed as potential antigens for the efficient detection of anti-MUC1 antibodies.

With this purpose, we established an indirect ELISA (Supporting Information) assay using both **P\*** and non-natural MUC1 **2fP\*** as coating antigens to detect anti-MUC1 antibodies from serum samples of patients with benign and malignant prostate tumors. As can be observed in Figure 7, the signal-to-noise ratio was statistically higher when **2fP\*** was used for both adenocarcinoma and benign hyperplasia. Our study also shows a higher concentration of anti-MUC1 antibodies in malignant tumors, which agrees with other assays conducted with breast tumor patients<sup>19</sup> and importantly validates our protocol. The results disclosed here demonstrate the potential application of the designed **2fP\*** MUC1 variant as a biomarker for improved detection of circulating anti-MUC1 antibodies in the serum of patients.

## CONCLUSIONS

A multidisciplinary approach to unravel key features of MUC1 recognition has been established. In particular, a new set of non-natural MUC1 derivatives comprising a (4S)-4-fluoro-L-proline or 4,4-difluoro-L-proline residue at the most immunogenic domain have been designed and synthesized. These compounds present a clear enhancement in the binding affinity against two anti-MUC1 antibodies with respect to the natural antigens. Both experimental X-ray studies and theoretical MD simulations confirm that, in agreement with our expectations, the hydrogen-by-fluorine substitution enhances the key CH/ $\pi$  interaction, which is crucial for improving the binding of the antigen to the antibody. Moreover, the obtained glycopeptides

display a significant potential as diagnostic tools to detect anti-MUC1 antibodies in prostate cancer patients.

## ■ ASSOCIATED CONTENT

### ● Supporting Information

The Supporting Information is available free of charge on the ACS Publications website at DOI: 10.1021/jacs.7b09447.

Characterization of the glycopeptides, biolayer interferometry fit obtained for the glycopeptides, microarray figures, details of the X-ray structure of  $\text{fP}^*$  bound to scFv-SM3, Cartesian coordinates, electronic energies, and lowest frequencies of the DFT calculated structures, additional molecular dynamics simulation figures, protocol of the ELISA, and details of the human sera samples (PDF)

## ■ AUTHOR INFORMATION

### Corresponding Authors

\*francisco.corzana@unirioja.es

\*gb453@cam.ac.uk; gbernardes@medicina.ulisboa.pt

### ORCID

Víctor J. Somovilla: 0000-0001-5067-6568

Fayna García-Martín: 0000-0001-9118-3874

Shin-Ichiro Nishimura: 0000-0002-6608-8418

Jesús Jiménez-Barbero: 0000-0001-5421-8513

Jesús H. Busto: 0000-0003-4403-4790

Jesús M. Peregrina: 0000-0003-3778-7065

Gonçalo J. L. Bernardes: 0000-0001-6594-8917

Francisco Corzana: 0000-0001-5597-8127

### Author Contributions

□ V. J. Somovilla, I. A. Bermejo, and I. S. Albuquerque have contributed equally.

### Notes

The authors declare no competing financial interest.

## ■ ACKNOWLEDGMENTS

We thank the Ministerio de Economía y Competitividad (projects CTQ2015-67727-R, UNLR13-4E-1931, CTQ2013-44367-C2-2-P, CTQ2015-64597-C2-1P, and BFU2016-75633-P). I.A.B. thanks the Asociación Española Contra el Cáncer en La Rioja for a grant. I.S.A. and G.J.L.B. thank FCT Portugal (Ph.D. studentship and FCT Investigator, respectively) and EPSRC. G.J.L.B. holds a Royal Society URF and an ERC StG (TagIt). F.C. and G.J.L.B. thank the EU (Marie-Sklodowska Curie ITN, Protein Conjugates). R.H.G. thanks Agencia Aragonesa para la Investigación y Desarrollo (ARAIID) and the Diputación General de Aragón (DGA, B89) for financial support. The research leading to these results has also received funding from the FP7 (2007-2013) under BioStruct-X (grant agreement no. 283570 and BIOSTRUCTX\_5186). We thank synchrotron radiation source DIAMOND (Oxford) and beamline I04 (number of experiment mx10121-19). The Hokkaido University group acknowledges JSPS KAKENHI grant no. 25220206 and JSPS Wakate B KAKENHI grant no. 24710242. We also thank CESGA (Santiago de Compostela) for computer support.

## ■ REFERENCES

(1) Taylor-Papadimitriou, J.; Burchell, J. M. *Mucins and Cancer*; Future Medicine Ltd: Unitec House, London, UK, 2013.

(2) Hollingsworth, M. A.; Swanson, B. J. *Nat. Rev. Cancer* **2004**, *4*, 45–60.

(3) Kufe, D. W. *Nat. Rev. Cancer* **2009**, *9*, 874–885.

(4) Kailemia, M. J.; Park, D.; Lebrilla, C. B. *Anal. Bioanal. Chem.* **2017**, *409*, 395–410.

(5) Adamczyk, B.; Tharmalingam, T.; Rudd, P. M. *Biochim. Biophys. Acta, Gen. Subj.* **2012**, *1820*, 1347–1353.

(6) Varela, J. C.; Atkinson, C.; Woolson, R.; Keane, T. E.; Tomlinson, S. *Int. J. Cancer* **2008**, *123*, 1357–1363.

(7) Rabassa, M. E.; Croce, M. V.; Pereyra, A.; Segal-Eiras, A. *BMC Cancer* **2006**, *6*, 253.

(8) Buskas, T.; Thompson, P.; Boons, G.-J. *Chem. Commun.* **2009**, *105*, 5335–5349.

(9) Wolfert, M. A.; Boons, G.-J. *Nat. Chem. Biol.* **2013**, *9*, 776–784.

(10) Wilson, R. M.; Danishefsky, S. J. *J. Am. Chem. Soc.* **2013**, *135*, 14462–14472.

(11) Gaidzik, N.; Westerlind, U.; Kunz, H. *Chem. Soc. Rev.* **2013**, *42*, 4421–4442.

(12) Richichi, B.; Thomas, B.; Fiore, M.; Bosco, R.; Qureshi, H.; Nativi, C.; Renaudet, O.; BenMohamed, L. *Angew. Chem., Int. Ed.* **2014**, *53*, 11917–11920.

(13) Blixt, O.; Bueti, D.; Burford, B.; Allen, D.; Julien, S.; Hollingsworth, M.; Gammerman, A.; Fentiman, I.; Taylor-Papadimitriou, J.; Burchell, J. M. *Breast Cancer Res.* **2011**, *13*, R25.

(14) Hamanaka, Y.; Suehiro, Y.; Fukui, M.; Shikichi, K.; Imai, K.; Hinoda, Y. *Int. J. Cancer* **2003**, *103*, 97–100.

(15) von Mensdorff-Pouilly, S.; Verstraeten, A. A.; Kenemans, P.; Snijdwint, F. G.; Kok, A.; Van Kamp, G. J.; Paul, M. A.; Van Diest, P. J.; Meijer, S.; Hilgers, J. *J. Clin. Oncol.* **2000**, *18*, 574–583.

(16) Tang, Z.-M.; Ling, Z.-G.; Wang, C.-M.; Wu, Y.-B.; Kong, J.-L. *PLoS One* **2017**, *12*, e0182117.

(17) Chen, H.; Werner, S.; Tao, S.; Zörnig, I.; Brenner, H. *Cancer Lett.* **2014**, *346*, 178–187.

(18) Tang, Y.; Cui, X.; Xiao, H.; Qi, S.; Hu, X.; Yu, Q.; Shi, G.; Zhang, X.; Gu, J.; Yu, Y.; Wang, L.; Li, Y. *Mol. Med. Rep.* **2017**, *15*, 2659–2664.

(19) Tang, Y.; Wang, L.; Zhang, P.; Wei, H.; Gao, R.; Liu, X.; Yu, Y.; Wang, L.; Wang, L. *Clin. Vaccine Immunol.* **2010**, *17*, 1903–1908.

(20) Gheybi, E.; Amani, J.; Salmanian, A. H.; Mashayekhi, F.; Khodi, S. *Tumor Biol.* **2014**, *35*, 11489–11497.

(21) Dokurno, P.; Bates, P. A.; Band, H. A.; Stewart, L. M.; Lally, J. M.; Burchell, J. M.; Taylor-Papadimitriou, J.; Snary, D.; Sternberg, M. J.; Freemont, P. S. *J. Mol. Biol.* **1998**, *284*, 713–728.

(22) Martínez-Sáez, N.; Castro-López, J.; Valero-González, J.; Madariaga, D.; Compañón, I.; Somovilla, V. J.; Salvadó, M.; Asensio, J. L.; Jiménez-Barbero, J.; Avenoza, A.; Busto, J. H.; Bernardes, G. J. L.; Peregrina, J. M.; Hurtado-Guerrero, R.; Corzana, F. *Angew. Chem., Int. Ed.* **2015**, *54*, 9830–9834.

(23) Karsten, U.; Serttas, N.; Paulsen, H.; Danielczyk, A.; Goletz, S. *Glycobiology* **2004**, *14*, 681–692.

(24) Her, C.; Westler, W. M.; Yang, T. *JSM Chem.* **2013**, *1*, 1004.

(25) Asensio, J. L.; Ardá, A.; Cañada, F. J.; Jiménez-Barbero, J. *Acc. Chem. Res.* **2013**, *46*, 946–954.

(26) Jiménez-Moreno, E.; Jiménez-Osés, G.; Gómez, A. M.; Santana, A. G.; Corzana, F.; Bastida, A.; Jiménez-Barbero, J.; Asensio, J. L. *Chem. Sci.* **2015**, *6* (11), 6076–6085.

(27) Hsu, C.-H.; Park, S.; Mortenson, D. E.; Foley, B. L.; Wang, X.; Woods, R. J.; Case, D. A.; Powers, E. T.; Wong, C.-H.; Dyson, H. J.; Kelly, J. W. *J. Am. Chem. Soc.* **2016**, *138*, 7636–7648.

(28) Hudson, K. L.; Bartlett, G. J.; Diehl, R. C.; Agirre, J.; Gallagher, T.; Kiessling, L. L.; Woolfson, D. N. *J. Am. Chem. Soc.* **2015**, *137*, 15152–15160.

(29) Zhao, Y.; Truhlar, D. G. *Theor. Chem. Acc.* **2008**, *120*, 215–241.

(30) Martínez-Sáez, N.; Supekar, N. T.; Wolfert, M. A.; Bermejo, I. A.; Hurtado-Guerrero, R.; Asensio, J. L.; Jiménez-Barbero, J.; Busto, J. H.; Avenoza, A.; Boons, G.-J.; Peregrina, J. M.; Corzana, F. *Chem. Sci.* **2016**, *7*, 2294–2301.

(31) Matsushita, T.; Takada, W.; Igarashi, K.; Naruchi, K.; Miyoshi, R.; Garcia-Martin, F.; Amano, M.; Hinou, H.; Nishimura, S.-I. *Biochim. Biophys. Acta, Gen. Subj.* **2014**, *1840*, 1105–1116.

(32) Coelho, H.; Matsushita, T.; Artigas, G.; Hinou, H.; Cañada, F. J.; Lo-Man, R.; Leclerc, C.; Cabrita, E. J.; Jiménez-Barbero, J.; Nishimura, S.-I.; Garcia-Martin, F.; Marcelo, F. *J. Am. Chem. Soc.* **2015**, *137*, 12438–12441.